Quenching of Spectroscopic Factors for Proton Removal in Oxygen Isotopes

Ø. Jensen,[1] G. Hagen,[2,3] M. Hjorth-Jensen,[1] B. Alex Brown,[4,5] and A. Gade[4,5]

[1]*Department of Physics and Center of Mathematics for Applications, University of Oslo, N-0316 Oslo, Norway*
[2]*Physics Division, Oak Ridge National Laboratory, Oak Ridge, Tennessee 37831, USA*
[3]*Department of Physics and Astronomy, University of Tennessee, Knoxville, Tennessee 37996, USA*
[4]*National Superconducting Cyclotron Laboratory, Michigan State University, East Lansing, Michigan 48824-1321, USA*
[5]*Department of Physics and Astronomy, Michigan State University, East Lansing, Michigan 48824, USA*

(Received 8 April 2011; published 11 July 2011)

We present microscopic coupled-cluster calculations of the spectroscopic factors for proton removal from the closed-shell oxygen isotopes ^{14,16,22,24,28}O with a chiral nucleon-nucleon interaction at next-to-next-to-next-to-leading order. We include coupling-to-continuum degrees of freedom by using a Hartree-Fock basis built from a Woods-Saxon single-particle basis. This basis treats bound and continuum states on an equal footing. We find a significant quenching of spectroscopic factors in the neutron-rich oxygen isotopes, pointing to enhanced many-body correlations induced by strong coupling to the scattering continuum above the neutron emission thresholds.

DOI: 10.1103/PhysRevLett.107.032501 PACS numbers: 21.10.Jx, 21.10.Gv, 21.60.De, 31.15.bw

The concept of independent particle motion, and mean-field approaches based thereupon, has played and continues to play a fundamental role in studies of quantum mechanical many-particle systems. From a theoretical standpoint, a single-particle (or quasiparticle) picture of states near the Fermi surface offers a good starting point for studies of systems with many interacting particles. For example, the success of the nuclear shell model rests on the assumption that the wave functions used in nuclear structure studies can be approximated by Slater determinants built on various single-particle states. The nuclear shell model assumes thus that protons and neutrons move as independent particles with given quantum numbers, subject to a mean field generated by all other nucleons. Deviations from such a picture have been interpreted as a possible measure of correlations. Indeed, correlations are expected to reveal important features of both the structure and the dynamics of a many-particle system beyond the mean-field picture.

In a field like nuclear physics, where the average density in nuclei is high and the interaction between nucleons is strong, correlations beyond the independent-particle motion are expected to play an important role in spectroscopic observables. Experimental programs in low-energy nuclear physics aim at extracting information at the limits of stability of nuclear matter. Correlations which arise when moving towards either the proton or the neutron dripline should then provide us with a better understanding of shell structure and single-particle properties of nuclei. So-called magic nuclei are particularly important for a fundamental understanding of single-particle states outside shell closures, with wide-ranging consequences spanning from our basic understanding of nuclear structure to the synthesis of the elements [1,2]. Unfortunately, the correlations in many-particle systems are very difficult to quantify experimentally and to interpret theoretically. There are rather few observables from which clear information on correlations beyond an independent particle motion in a nuclear many-body environment can be extracted.

A quantity which offers the possibility to study deviations from a single-particle picture, and thereby provide information on correlations, is the spectroscopic factor (SF). From a theoretical point of view they quantify what fraction of the full wave function can be interpreted as an independent single-particle or single-hole state on top of a correlated state, normally chosen to be a closed-shell nucleus. Although not being experimentally observable [3–5], the radial overlap functions, whose norm are the SFs, are required inputs to theoretical models for nucleon capture, decay, transfer and knockout reactions. There is a wealth of experimental data and theoretical analysis of such reactions for stable nuclei [1,6,7]. Data from $(e, e'p)$ experiments on stable nuclei [1] indicate that proton absolute SFs are quenched considerably with respect to the independent-particle model value, with short-range and tensor correlations assumed to be an important mechanism. Adding long-range correlations as well from excitations around the Fermi surface, one arrives at a quenching of 30%–40%, see, for example, Ref. [8]. Nuclear physics offers therefore a unique possibility, via studies of quantities like SFs, to extract information about correlations beyond mean-field in complicated, two-component, many-particle systems.

Recent data on knockout reactions on nuclei with large neutron-proton asymmetries indicate that the nucleons of the deficient species, being more bound, show larger reductions of spectroscopic strength than the less bound excess species [9,10]. It is the aim of this work to understand which correlations are important when one moves towards more weakly bound systems. For this, we study the

 © 2011 American Physical Society

chain of oxygen isotopes and compute SFs for proton removal from ^{14,16,22,24,28}O. These isotopes span a large range of proton-neutron asymmetries, from 4/3 in ^{14}O to 2/5 in ^{28}O. Using *ab initio* coupled-cluster theory described below [11], we argue that the reduction in SFs is due to many-body correlations arising from the coupling to the scattering continuum in neutron-rich oxygen isotopes. After these introductory remarks, we give a brief overview of our formalism, before presenting our results and conclusions.

The spectroscopic factor $S^A_{A-1}(lj) = |O^A_{A-1}(lj;r)|^2$, is the norm of the overlap function,

$$O^A_{A-1}(lj;r) = \sum\!\!\!\!\!\!\int_n \langle A-1||\tilde{a}_{nlj}||A\rangle \phi_{nlj}(r). \qquad (1)$$

Here, $O^A_{A-1}(lj;r)$ is the radial overlap function of the many-body wave functions for the two independent systems with A and $A-1$ particles, respectively. In this work we consider only overlaps with $|A\rangle$ in the ground state. The double bar denotes a reduced matrix element, and the integral-sum over n represents both the sum over the discrete spectrum and an integral over the corresponding continuum part of the spectrum. The annihilation operator $\tilde{a}_{nlj}$ is a spherical tensor of rank j. The radial single-particle basis function is given by the term $\phi_{nlj}(r)$, where l and j denote the single-particle orbital and angular momentum, respectively, and n is the nodal quantum number. The isospin quantum number has been suppressed. We emphasize that the overlap function, and hence also its norm, is defined microscopically and independently of the single-particle basis. It is uniquely determined by the many-body wave functions $|A\rangle$ and $|A-1\rangle$. From the definition of the overlap function in Eq. (1) it is clear that the SF is mainly a measure of how well nucleus A can be described by a single, uncorrelated nucleon attached to nucleus $A-1$. Large deviations from unity indicate an increased role of many-body correlations beyond a mean-field picture. For calculational details see Ref. [12].

We use the coupled-cluster (CC) ansatz [11] $|\psi_0\rangle = \exp(T)|\phi_0\rangle$ for the ground states of the closed-shell oxygen isotopes ^{14,16,22,24,28}O. The reference state, $|\phi_0\rangle$, is an antisymmetric product state for all A nucleons. The cluster operator T introduces correlations as a linear combination of particle-hole excitations $T = T_1 + T_2 + \ldots + T_A$, where T_n represents an n-particle-n-hole excitation operator. For the CC singles and doubles approximation (CCSD) employed in this work, T is truncated at the level of double excitations, $T = T_1 + T_2$.

Because of the non-Hermiticity of the standard CC formalism, we need to calculate both the left and the right eigenvectors. These are determined via the equation-of-motion CC (EOM-CC) approach as $|A\rangle \approx |R^A_\nu(J_A)\rangle \equiv \exp(T)R^A_\nu(J_A)|\phi_0\rangle$ and $\langle A| \approx \langle L^A_\nu(J_A)| \equiv \langle\phi_0|L^A_\nu(J_A)\times \exp(-T)$. The operators $R^A_\nu(J_A)$ and $L^A_\nu(J_A)$ produce linear combinations of particle-hole excited states when acting to the right and left, respectively. In the spherical form of the EOM-CC approach, the operators have well-defined angular momentum by construction, as indicated by J_A, which stands for the angular momentum considered. If the A-body system is in its ground state, the right EOM-CC wave function is identical to the CC ground state.

Solutions for the $(A-1)$-body systems are obtained with particle-removed equation-of-motion coupled-cluster method, truncated at the level of 2-hole-1-particle excitations. Here, we use the CCSD ground state solution of the closed-shell nucleus A as the reference state in order to determine the corresponding left and right eigenvectors $|A-1\rangle \approx |R^{A-1}_\mu(J_{A-1})\rangle \equiv \exp(T)R^{A-1}_\mu(J_{A-1})|\phi_0\rangle$ and $\langle A-1| \approx \langle L^{A-1}_\mu(J_{A-1})| \equiv \langle\phi_0|L^{A-1}_\mu(J_{A-1})\exp(-T)$. In actual calculations, the EOM-CC wave functions are obtained by determining the operators $R^A_\nu(J_A)$ and $L^A_\nu(J_A)$ as eigenvectors of the similarity-transformed Hamiltonian, $\bar{H} = \exp(-T)H\exp(T)$. We refer the reader to Refs. [11,13,14] for details about EOM-CC.

Finally, we can write the SF in the spherical CC formalism as

$$S^A_{A-1}(lj) = \sum\!\!\!\!\!\!\int_n \langle L^{A-1}_\mu(J_{A-1})||\overline{\tilde{a}_{nlj}}||R^A_\nu(J_A)\rangle \times \langle R^{A-1}_\mu(J_{A-1})||\overline{\tilde{a}_{nlj}}||L^A_\nu(J_A)\rangle^*, \qquad (2)$$

where we have used the similarity-transformed spherical annihilation operator defined in Ref. [12]. The labels μ and ν are included to distinguish between states in $|A\rangle$ and $|A-1\rangle$.

The intrinsic A-nucleon Hamiltonian reads $\hat{H} = \hat{T} - \hat{T}_{\rm cm} + \hat{V}$, where $\hat{T}$ is the kinetic energy, $\hat{T}_{\rm cm}$ is the kinetic energy of the center-of-mass coordinate, and $\hat{V}$ is the two-body nucleon-nucleon (NN) interaction. We employ here the N^{3}LO model of Entem and Machleidt [15]. This interaction model is constructed with a cutoff of $\Lambda = 500$ MeV. Calculations starting from this Hamiltonian have been shown to generate CC solutions that are separable into a Gaussian center-of-mass wave function and an intrinsic wave function, see, for example, Refs. [14,16].

We use a Hartree-Fock (HF) solution for the reference state, as detailed in, for example, Ref. [13]. These HF solutions were built from the standard harmonic oscillator (HO) basis combined with Woods-Saxon (WS) single-particle bound- and scattering states for selected partial waves. The role of the continuum is expected to be important close to the dripline, as seen in Refs. [13,17,18]. For this purpose we use a spherical WS basis for the neutron $s_{1/2}$, $d_{3/2}$, and $d_{5/2}$ partial waves. The single-particle bound and scattering states are obtained by diagonalizing a one-body Hamiltonian with a spherical Woods-Saxon potential defined on a discretized set of real momenta. We employ a total of 30 mesh points along the real momentum axis for each of the $s_{1/2}$, $d_{3/2}$, and $d_{5/2}$ neutron partial waves. For the harmonic oscillator basis we

included all single-particle states spanned by 17 major oscillator shells.

Figure 1 shows the calculated SFs for removing a proton in the $p_{1/2}$ and $p_{3/2}$ partial waves of ^{14,16,22,24,28}O. We compare our calculations of the SFs to calculations using an HF basis built entirely from harmonic oscillator basis functions (HF-OSC, dashed lines). The results are obtained with an harmonic oscillator energy $\hbar\omega = 30$ MeV. Our calculations of the SFs depend weakly on the harmonic oscillator frequency, see, for example, Ref. [12]. The $p_{1/2}$ and $p_{3/2}$ proton orbitals are close to the Fermi level. In a traditional shell-model picture we would therefore expect SFs close to unity for such states. However, we find a significant quenching of the SFs due to the coupling-to-continuum degrees of freedom. The calculations done with a HF-OSC basis show no significant quenching, and illustrate clearly the limitation of the harmonic oscillator basis representation of weakly bound, neutron-rich nuclei. This observation agrees also nicely with the analysis of Michel *et al.* [19]. There, the authors demonstrate that the energy dependence of SFs due to an opening of a reaction channel can only be described properly in shell-model calculations if correlations involving scattering states are treated properly.

In our calculations the closed-shell oxygen isotopes ^{14,16,22,24,28}O are all bound with respect to neutron emission (for this particular N^{3}LO interaction with cutoff $\Lambda =$ 500 MeV). In particular, we get ^{28}O bound by 3.67 MeV with respect to one-neutron emission. However, starting from an N^{3}LO interaction with a cutoff $\Lambda = 600$ MeV, we get ^{28}O unbound with respect to four-neutron emission and ^{24}O, as seen in Ref. [20]. To judge the theoretical basis for the demonstrated continuum effect, we also computed SFs for the proton removal from ^{14,16,22}O using the $\Lambda =$ 600 MeV N^{3}LO interaction model. We found similar results as for the $\Lambda = 500$ MeV N^{3}LO interaction model, and conclude that the theoretical uncertainties related to short-range correlations do not seem to impair the results reported here.

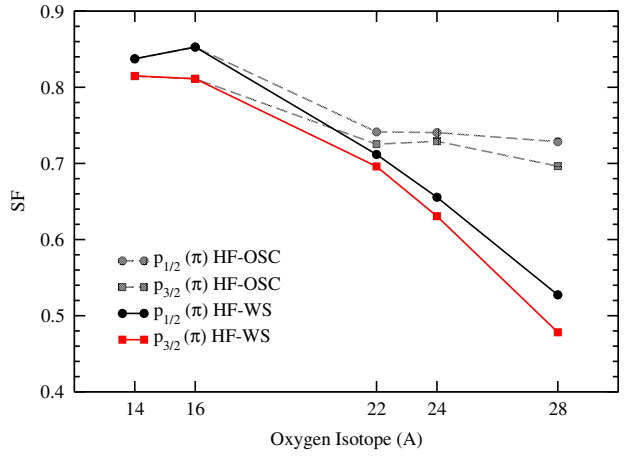

FIG. 1 (color online). Normalized spectroscopic factors for $p_{1/2}$ and $p_{3/2}$ proton removal from the oxygen isotopes ^{14,16,22,24,28}O. The continuum states included in the calculation (HF-WS) lead to a dramatic quenching of the spectroscopic factors as the neutron dripline is approached. For comparison, we show calculations of spectroscopic factors using a HF basis built entirely from harmonic oscillator basis functions (HF-OSC).

To further understand the role of correlations beyond mean-field we compared the SF for $p_{1/2}$ proton removal from ^{24}O for three different approximations to $|A\rangle$ and $|A-1\rangle$. To get bound solutions for ^{24}O in simpler calculation schemes, we softened the N^{3}LO interaction through similarity renormalization group (SRG) methods [21]. For each approximation we considered three values of the SRG flow parameter $\lambda = 3.2, 3.4, 3.6$ fm^{-1}. First, in the crudest approximation, using a mean-field HF solution for $|A\rangle$ and $|A-1\rangle$, the SFs are by definition equal to unity. Secondly, we used a HF solution for $|A\rangle$ while $|A-1\rangle$ was approximated by one-hole and two-hole-one-particle excitations on the HF ground state $|A\rangle$. In this case we observed about 15%–20% reduction in the SFs. Finally, our EOM-CC approach in Eq. (2), gave a reduction of 20%–25% over the range of λ considered. This clearly shows the importance of correlations beyond the mean-field. Varying the SRG flow parameter from 3.2 fm^{-1} to 3.6 fm^{-1} we found that the SFs varied from 0.79 to 0.75, illustrating the role of short-range correlations.

The shape of the calculated overlap functions reveals more information. In order to probe the sensitivity of the tail of the overlap functions as we move towards ^{28}O, we compute the ratios of the absolute square of the radial overlap functions to the $|\langle^{15}\mathrm{N}|a_{lj}|^{16}\mathrm{O}\rangle|^2$ radial overlap function. These results are shown in Fig. 2 for the $p_{1/2}$ proton state (the $p_{3/2}$ proton state shows a very similar pattern). A notable reduction of these norms towards more neutron-rich nuclei is seen. The downward dip of the

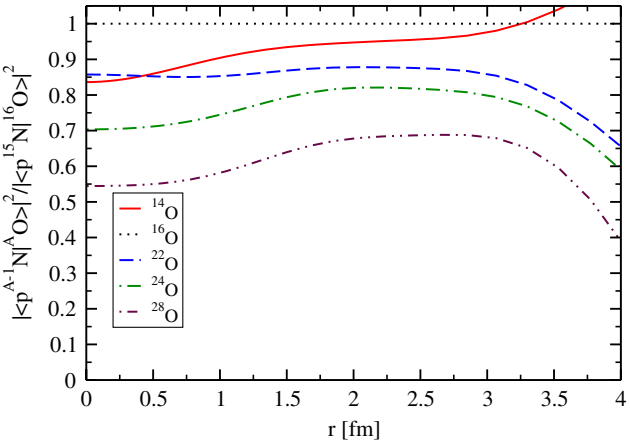

FIG. 2 (color online). Ratio of the radial overlap functions $\langle^{13}\mathrm{N}|a_{lj}|^{14}\mathrm{O}\rangle$, $\langle^{15}\mathrm{N}|a_{lj}|^{16}\mathrm{O}\rangle$, $\langle^{21}\mathrm{N}|a_{lj}|^{22}\mathrm{O}\rangle$, $\langle^{23}\mathrm{N}|a_{lj}|^{24}\mathrm{O}\rangle$, and $\langle^{27}\mathrm{N}|a_{lj}|^{28}\mathrm{O}\rangle$ for the $p_{1/2}$ single-particle state.

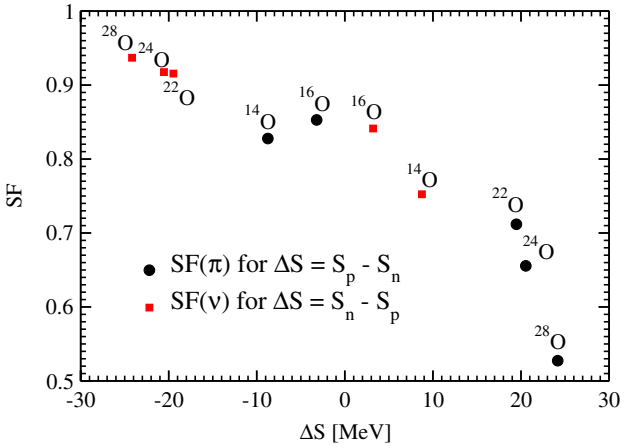

FIG. 3 (color online). Plot of calculated SFs as functions of the difference between the calculated neutron and proton separation energies. The results are for the single-particle states closest to the Fermi surface. For protons these are the $p_{1/2}$ states.

overlap ratios at larger radii comes from the fact that the $p_{1/2}$ proton orbital become more and more bound as more neutrons are added to ^{16}O. For ^{14}O the $p_{1/2}$ proton is less bound with respect to ^{16}O, resulting in a bend upward. As we approach the neutron dripline, the one-neutron emission thresholds for the oxygen isotopes and their neighboring nitrogen isotopes get closer to the scattering threshold. Clearly, the tail of the wave functions will play a more important role as the outermost neutrons get closer to the scattering threshold. It is exactly this effect we observe in our calculations of the SFs for proton removal. Using a HF basis of purely harmonic oscillator wave functions, the density in the interior region of the nucleus is overestimated, while the density is shifted towards the tail when using a basis with correct asymptotic behavior. One should note that the nitrogen isotopes for a given neutron number are more loosely bound than their corresponding oxygen isotones, and this is the essential reason for the reduction. For ^{28}O and ^{27}N, no experimental values are available but if ^{28}O exists it will be very loosely bound and we may assume that ^{27}N is unbound.

Finally, we show in Fig. 3 the SFs of the proton and neutron states closest to the Fermi surface (for protons the $p_{1/2}$-state), as a function of the difference between the computed proton and neutron separation energies. The results here agree excellently with similar interpretations made in Refs. [9,10]. One sees clearly an enhancement of correlations for the strongly bound, deficient nucleon species with increasing asymmetry.

In conclusion, we have found a large quenching of the spectroscopic factors for the deeply-bound proton states near the Fermi surface in the neutron-rich oxygen isotopes. This can be ascribed mainly to many-body correlations arising from a proper treatment of neutron scattering states. These results agree nicely with the mathematical analysis performed by Michel *et al.* [19]. This result for the oxygen isotopes is similar to what has been inferred from neutron knockout reaction cross sections for deeply-bound neutron states near the Fermi surface in proton-rich *sd*-shell nuclei [9,10]. Clearly, more work is needed to confirm the connection; experiments for proton knockout from oxygen should be undertaken and many-body calculations for proton-rich, heavy nuclei need to be carried out.

We thank Marek Płoszajczak for useful comments. This work was supported by the Office of Nuclear Physics, U. S. Department of Energy (Oak Ridge National Laboratory); the University of Washington under Contract No. DE-FC02-07ER41457 and NSF Grant No. PHY-0758099. This research used computational resources of the National Center for Computational Sciences and the Notur project in Norway.

[1] V. R. Pandharipande, I. Sick, and P. K. A. deWitt Huberts, Rev. Mod. Phys. **69**, 981 (1997).
[2] K. L. Jones *et al.*, Nature (London) **465**, 454 (2010).
[3] R. J. Furnstahl and H. W. Hammer, Phys. Lett. B **531**, 203 (2002).
[4] A. M. Mukhamedzhanov and A. S. Kadyrov, Phys. Rev. C **82**, 051601(R) (2010).
[5] B. K. Jennings, arXiv:1102.3721.
[6] C. Barbieri, Phys. Rev. Lett. **103**, 202502 (2009).
[7] J. Lee, M. B. Tsang, W. G. Lynch, M. Horoi, and S. C. Su, Phys. Rev. C **79**, 054611 (2009).
[8] W. H. Dickhoff and C. Barbieri, Prog. Part. Nucl. Phys. **52**, 377 (2004).
[9] A. Gade *et al.*, Phys. Rev. C **77**, 044306 (2008).
[10] A. Gade *et al.*, Phys. Rev. Lett. **93**, 042501 (2004).
[11] I. Shavitt and R. J. Bartlett, *Many-Body Methods in Chemistry and Physics*, (Cambridge University Press, Cambridge, England, 2009).
[12] Ø. Jensen, G. Hagen, T. Papenbrock, D. J. Dean, and J. S. Vaagen, Phys. Rev. C **82**, 014310 (2010); Ø. Jensen, G. Hagen, M. Hjorth-Jensen, and J. S. Vaagen, Phys. Rev. C **83**, 021305(R) (2011).
[13] G. Hagen, T. Papenbrock, and M. Hjorth-Jensen, Phys. Rev. Lett. **104**, 182501 (2010).
[14] G. Hagen, T. Papenbrock, D. J. Dean, and M. Hjorth-Jensen, Phys. Rev. C **82**, 034330 (2010).
[15] D. R. Entem and R. Machleidt, Phys. Rev. C **68**, 041001 (R) (2003).
[16] G. Hagen, T. Papenbrock, and D. J. Dean, Phys. Rev. Lett. **103**, 062503 (2009).
[17] N. Michel, W. Nazarewicz, M. Płoszajczak, and T. Vertse, J. Phys. G **36**, 013101 (2009).
[18] A. Volya and V. Zelevinsky, Phys. Rev. C **74**, 064314 (2006).
[19] N. Michel, W. Nazarewicz, and M. Płoszajczak, Phys. Rev. C **75**, 031301 (2007); Nucl. Phys. **A794**, 29 (2007).
[20] G. Hagen, T. Papenbrock, D. J. Dean, M. Hjorth-Jensen, and B. V. Asokan, Phys. Rev. C **80**, 021306(R) (2009).
[21] S. K. Bogner, R. J. Furnstahl, and R. J. Perry, Phys. Rev. C **75**, 061001 (2007).